ACS APPLIED POLYMER MATERIALS

pubs.acs.org/acsapm Letter

Optically Transparent Polymer Aerogels Via Controlled Radical Polymerization

Stephen M. Meckler, Gabriel Iftime, Asritha Nallapaneni, Quentin Van Overmeere, Barkev Keoshkerian, Eli Bulger, Alec S. Ho, Chenhui Zhu, Jessy B. Rivest, and Mahati Chintapalli*

Cite This: *ACS Appl. Polym. Mater.* 2022, 4, 1565−1569 Read Online

ACCESS | Metrics & More | Article Recommendations | Supporting Information

ABSTRACT: We present a class of porous polymer monoliths with high visible light transmittance and low haze synthesized using nitroxide-mediated stable free radical polymerization (SFRP), a form of controlled radical polymerization, to suppress large pore structures. Such materials can find applications in thermally insulated windows. Aerogels with adjustable optical and pore properties were achieved by modulating the nitroxide radical equilibrium. Controlled radical polymerization resulted in materials with average pore widths <10 nm, porosities of 43%, and high visible transmittance >60% (for 2.8 mm thickness). These results provide general design rules for radical polymerization of clear, colorless porous polymers.

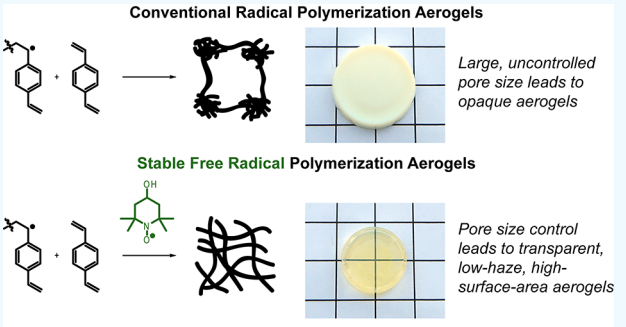

KEYWORDS: *aerogels, mesoporous materials, controlled radical polymerization, transparency, insulation, polymer*

Due to visible light scattering[1,2] in mesoporous materials (pore sizes 2−50 nm), high porosity and transparency with low haze are typically incompatible attributes. Polymers exhibiting high porosity while maintaining the optical transparency of a dense plastic could enable advanced applications such as thermally insulated windows that can address the 3.6 quadrillion Btu thermal energy lost through windows in the United States each year.[3] Low-cost transparent aerogel insulation could find a host of applications in glazings including daylighting and skylights, single-pane retrofits, storm windows, and thin double- and triple-pane insulated glazing units. Materials suitable for single pane window retrofits are particularly attractive because replacing existing single pane windows with modern, energy-efficient double pane windows has a prohibitively long payback period. Beyond buildings, additional applications for transparent, scalable, porous materials could certainly be contemplated. Such materials are elusive today because light scattering in porous materials is a strong function of scatterer size, with scattering arising from inhomogeneities in refractive index on the subwavelength scale.[4,5] High visible transparency at thicknesses relevant for thermal insulation applications (few mm) demands that pore features are <∼10 nm in diameter, which is not possible with existing scalable technologies.[2,4,6] We introduce a method to achieve transparency in mesoporous polymers through unprecedented control of pore and aggregate size in radical polymers.

The transparent polymer aerogels reported here have several advantages over the state-of-the-art silica aerogels and mesoporous polymers. While silica aerogels have high porosities, they exhibit a characteristic blue haze, are unstable to ambient moisture, and require expensive supercritical CO_2 drying unless subjected to additional process steps.[2,7−9] In contrast, the polydivinylbenzene (PDVB) materials in this study are intrinsically hydrophobic and can withstand ambient drying. Polymer aerogels are an emerging class of materials promising for aerospace, optoelectronic, and composite applications.[10] While most polymer aerogels are visible light absorbing and opaque due to scattering,[11] recent reports demonstrate transparent, albeit yellow, polyimide polymer aerogels.[10] No existing mesoporous polymers offer simultaneous porosity, transparency, and colorlessness.

We present design rules to access a class of transparent materials through the scalable controlled radical polymerization of a model high-cross-link-density polymer, PDVB. Key to our success is using SFRP to modulate chain growth and precipitation of nanogel clusters during polymerization. Conventional mesoporous PDVB from radical polymerization (RP) is opaque due to the formation of large nanogel clusters, in part due to chain−chain termination in growing nanogels that become linked in late polymerization (Scheme 1a) to produce large pore walls and cavities.[12] In an SFRP gelation

Received: December 23, 2021
Accepted: January 18, 2022
Published: February 8, 2022

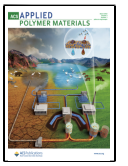

Scheme 1. Influence of SFRP on Gel Network Evolution[a]

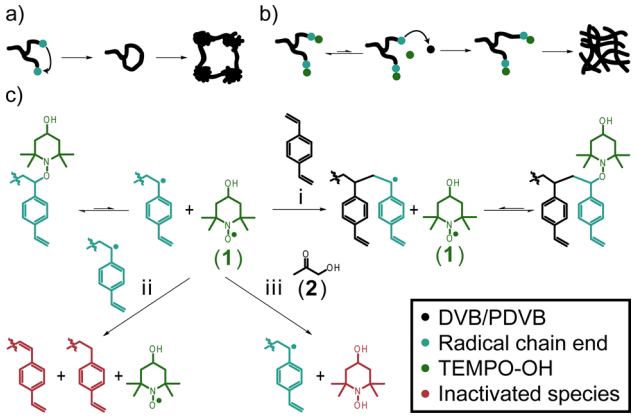

[a]Cartoons of (a) a conventional RP reaction and (b) an SFRP reaction. (c) Prominent chemical reactions dictating SFRP network growth include (i) nitroxide mediated chain growth, (ii) chain termination events such as hydrogen abstraction, and (iii) consumption of excess nitroxide mediator by reducing agent **2**.[13,16]

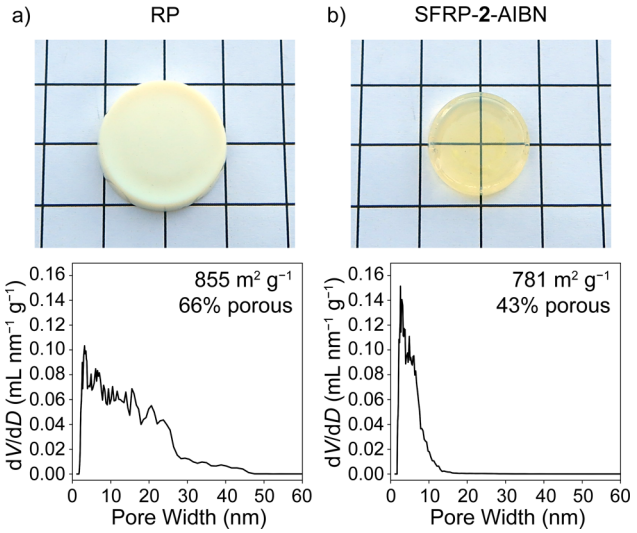

Figure 1. Pore size control via SFRP enables aerogels with enhanced transparency. Top row: photographs of typical (a) RP and (b) SFRP-**2**-AIBN aerogels. Grid lines are 1 cm apart. Bottom row: Typical NLDFT PSDs fit to N_2 adsorption isotherms at 77 K along with the specific surface areas and porosities.

reaction, we expect more homogeneous gels with smaller pore walls and cavities (Scheme 1b). In SFRP, a nitroxide mediator reversibly binds to growing chain ends, producing a "dormant" state.[13] Chain growth occurs only when nitroxide mediator **1** (TEMPO−OH) decouples from the chain end (Scheme 1c, pathway i). As the majority of chains are dormant, the reaction proceeds as a living polymerization with lowered probability of undesirable chain termination events. Ide et al. showed in solvated gels that in controlled polymerizations with cross-linking species, lower concentrations of active radicals suppress intrachain reactions in early stages of polymerization, reducing the formation of large, dense nanogel precipitates.[14,15]

Although many chain termination events are suppressed by the nitroxide mediator, hydrogen abstraction (Scheme 1c pathway ii) and chain−chain coupling still occur over time, leading to an excess of free nitroxide that effectively arrests polymerization.[13,16,17] Previous studies in simple, linear polymerizations have shown that the addition of a reducing agent such as 1-hydroxy-2-propanone (or acetol, **2**) slowly consumes excess nitroxide, producing a living polymerization throughout monomer incorporation (Scheme 1c, pathway iii).[16] Similarly, using a longer-half-life radical initiator, dicumyl peroxide (DCP), in conjunction with azobis(isobutyronitrile) (AIBN) has been shown to counter the accumulation of excess free nitroxide.[18] DCP introduces radicals gradually throughout the reaction, maintaining the ratio of propagating radicals to nitroxide.

We show here that in aerogel synthesis via cross-linking SFRP polymerizations the amount of excess free nitroxide controls nanogel formation and concomitant pore structure. To illustrate this, we prepared a series of PVDB samples of varying polymerization activity, which we define qualitatively as the reduction in excess free nitroxide relative to the SFRP reaction with no additives. The trend from most active polymerization to least is RP > SFRP with reducing agent and mixed initiator (SFRP-**2**-DCP/AIBN) > SFRP with reducing agent (SFRP-**2**-AIBN) > SFRP with no additives (SFRP-AIBN). In this series, SFRP-**2**-AIBN provides an exceptional balance of porosity and transparency. Full sample information including synthesis and characterization can be found in the Supporting Information (Tables S1 and S2 and Figures S1−S5).

Common to all reactions is the monomer, 80% divinylbenzene (DVB; 80% pure with a balance of ethylvinylbenzene), *N*-methylpyrrolidinone (NMP) as a solvent and porogen at 80% by volume, and AIBN as a radical initiator. The RP reactions were carried out at 90 °C for 1 h and the SFRP reactions at 125 °C for 48 h to promote reversibility of the radical equilibrium.[19] After gelation, the samples underwent solvent exchange followed by gradual ambient drying. Slow drying is essential to reduce gel cracking and improve the resultant mechanical properties. Due to the ambient drying processes employed with some change to the polymer network, these aerogels could also be categorized as xerogels.

SFRP aerogels demonstrate smaller pore size and higher transparency than RP aerogels while retaining 43% porosity (Figure 1), demonstrating the promise of SFRP aerogels as thermally insulated windows. Table 1 summarizes the results. In RP, a significant fraction of the porosity occurs at pore widths greater than 20 nm, as observed in the nonlocal density functional theory (NLDFT) pore size distribution, and the aerogel is fully opaque (Figure 1). The RP bulk porosity is

Table 1. Summary of Formulations Used to Produce the Aerogels in Figure 1 and Typical Resultant Pore Network and Optical Properties

Sample	AIBN[a]	TEMPO−OH (**1**)[a]	acetol (**2**)[a]	k_{95}/nm	d/nm	% porosity	% transmittance	% haze
RP	1	0	0	34	81	66	8.1	84.6
SFRP-**2**-AIBN	1	0.95	9.5	10	36	43	61.8	8.8

[a]1 equiv = 2.84 × 10^{-2} mmol of each compound added to 1 g of 20 wt % DVB in NMP.

https://doi.org/10.1021/acsapm.1c01854
ACS Appl. Polym. Mater. 2022, 4, 1565−1569

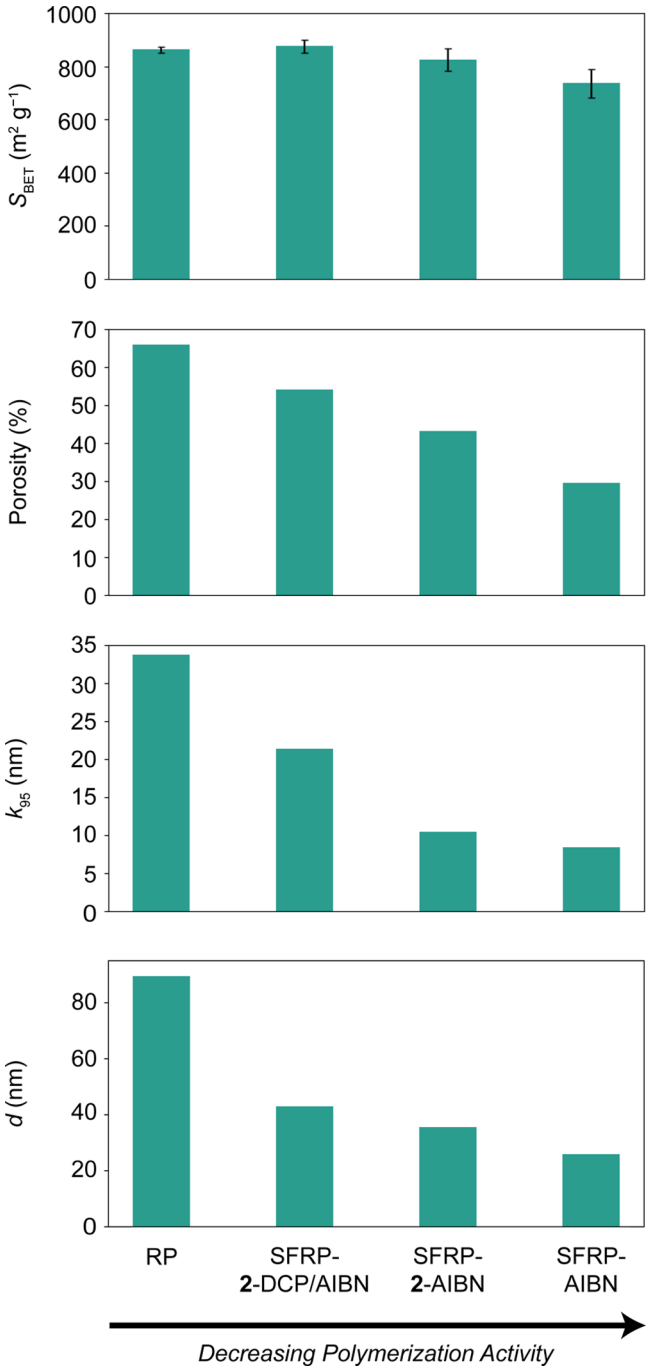

Figure 2. Comparison between relative polymerization activity and structural properties. S_{BET} (specific surface area), porosity, and k_{95} (pore size at 95% cumulative pore volume) are from N_2 adsorption, and particle size d is determined using SAXS. Error bars on the S_{BET} graph represent one standard deviation from the mean of three measurements, and all other measurements are from typical samples. Porosity, k_{95}, and d decrease monotonically with decreasing polymerization activity, but S_{BET} exhibits a more complex relation to activity.

66%, close to the 80 vol % of porogenic NMP in the formulation. In SFRP-**2**-AIBN, fully transparent aerogels were achieved with transmittance >60% and haze <10% (for 2.8 mm thickness). The optical properties are enabled by pores that are almost entirely <10 nm wide. SFRP-**2**-AIBN has a porosity of 43%, over half of the 80 vol % NMP. Some light is absorbed,

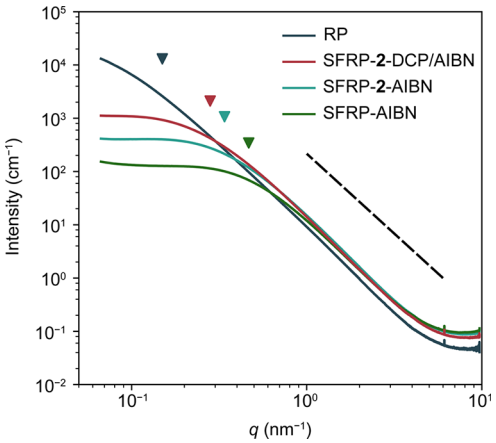

Figure 3. Intensity-calibrated SAXS profiles from porous polymers. The arrows point to the q values at the slope transitions used to calculate d, and the dashed line represents the slope for a Porod exponent of 3.

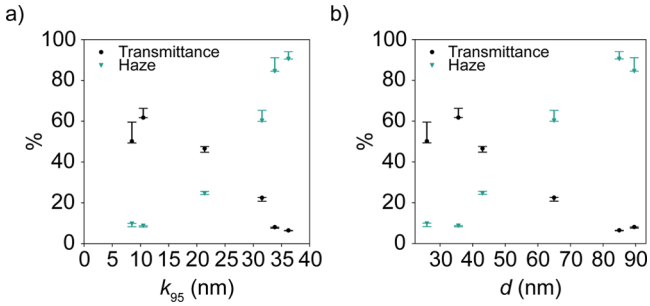

Figure 4. Transmittance and haze (2.8 mm thickness) of six aerogels plotted as a function of k_{95} and d. Error bars represent the range between the raw measured transmittance or haze value and the thickness corrected value accounting also for the standard deviation in the thickness measurement of the sample. Transmittance decreases and haze increases with increasing k_{95} and d.

resulting in a yellow hue; this is attributed to oxidation of the NMP solvent and styrenic monomers. Due to the flexibility of the SFRP platform, various monomers (e.g., styrenes, (meth)-acrylates, etc.) successfully formed aerogels, and oxidation-resistant monomers can be substituted to avoid coloration. An example of a colorless SFRP dry gel is included in the Supporting Information (Figure S6).

In principle, differences in pore size, nanogel particle size, and shrinkage can all account for the optical differences between SFRP and RP aerogels. However, in the solvated state, when solvent occupies 80 vol % in all samples, the RP and SFRP-2-AIBN gels appear opaque and transparent, respectively. Additionally, a high activity sample formulated for high porosity (SFRP-HP) demonstrates equivalent total porosity to RP but a transmittance nearly 3-fold higher (Table S2). Shrinkage alone cannot account for the transparency of SFRP samples.

We investigated the relationship between polymerization activity and polymer structure. Activity-dependent processes such as nanogel formation and nanogel interconnection impact both pore structure and polymer network structure. Correlations between pore characteristics determined via N_2 adsorption porosimetry and activity are shown in Figure 2. The porosity and k_{95} (the pore size at which the cumulative pore volume reaches 95%) decrease with diminishing activity of the

https://doi.org/10.1021/acsapm.1c01854
ACS Appl. Polym. Mater. 2022, 4, 1565−1569

formulation. The k_{95} value is a convenient measure of the pore size as it is biased toward pores with large light scattering cross sections. The surface area, S_{BET}, of the sample follows a similar trend but is not monotonic. Because S_{BET} decreases with decreasing porosity but increases with decreasing pore size, the relationship is driven by competing forces.

Polymer network properties, determined via small-angle X-ray scattering (SAXS, Advanced Light Source synchrotron, Berkeley CA, 7.3.3),[20] also correlate with activity. Scattering profiles of four samples are shown in Figure 3. Intensity-calibrated scattering data is plotted against scattering vector, q, where $q = 4\pi \sin(\theta)/\lambda$, θ is scattering angle, and λ is X-ray wavelength. From the scattering profiles, the slope at high q indicates the Porod exponent, p. In all samples, $4 > p > 3$, indicating a surface fractal structure, with the actual values ranging from 3.1−3.3 (Figure S7). Based on the p-values, the aerogels are networks of rough primary particles, rather than networks of smooth nonfractal particles ($p \sim 4$) or networks of polymer segments (mass fractal, $p < 3$).[21] Samples with lower activity (more "living") have lower values of p, indicating primary particles that are rougher and more branched, and closer to mass fractals. The observed change in fractal dimension is qualitatively consistent with the mechanism depicted in Scheme 1a,b. The characteristic particle size, d, is estimated from the q-value at the slope change between the Porod and low-q regions ($q \sim 0.1$−0.3 nm^{-1}). Particle size decreases from 81 nm for RP to 26 nm for SFRP-AIBN; thus, decreasing activity correlates with smaller d (Figure 2). We posit that d arises from nanogel clusters formed in early stages of polymerization, which are of comparable size.[14] Furthermore, the particle sizes from SEM images of SFRP-**2**-AIBN are consistent with d from SAXS (Figure S8).

Our trends in gel structure with activity are supported by reports that controlled radical polymerization suppresses nanogel formation compared to RP.[14,15] Less active polymerizations have smaller d and p, indicating rougher and smaller nanogel particles, consistent with the higher surface area at equivalent porosity, pore size distributions with lower k_{95}, and lower porosity due to higher shrinkage observed via N_2 adsorption. The smaller k_{95} is a result of smaller spacing between nanogel clusters in addition to higher shrinkage. By modulating polymerization activity via the excess free nitroxide, we have demonstrated a method to tune the size of the nanogels, reaching nanogel sizes not accessible by RP.[12]

Control of polymer and pore structure dictates aerogel optical properties. In Figures 4 and S8, relationships between structure characteristics and optical properties are shown for the four formulations with varying activity and two additional high activity formulations (Tables S1 and S2). Figure 4 shows that transmittance decreases and haze increases nearly monotonically with both k_{95} and d. These correlations are consistent with that the fact that large pores and pore walls have larger scattering cross sections.[4] The same haze and transmittance measurements have a more complex dependence on porosity (Figure S9). Recently Zhao et al. and others have shown that optical properties depend on a combination of pore size, porosity, and particle size.[2,4,6]

In unpublished experiments, polymerization activity did not significantly impact mechanical properties, quantified via compressive modulus; regardless of polymerization, modulus vs porosity follows the same (linear) relationship.

We have demonstrated a method to rationally design the pore structure and optical properties of mesoporous polymers by tuning the degree of control in a living radical polymerization. Relative to RP, SFRP increases transmittance and decreases haze via changes to both polymer network and pore structure. We demonstrated a material suitable for transparent thermal insulation applications with >60% transmittance, <10% haze (2.8 mm thick), and porosity of 43%. The thermal conductivity of a larger sample analogous to SFRP-**2**-AIBN was measured to be 0.09 W/mK, 1.5−3× lower than typical engineering polymers (see Supporting Information).[22] Relaxing the requirement for transparency, we note that high activity SFRP can also lead to mesoporous materials with unusually high S_{BET}, >900 m^2/g (Table S2), relative to other 1-step, primary cross-linking reactions. Our design rules are generalizable to the large class of materials compatible with the range of controlled polymerizations (e.g., ATRP, RAFT). Expanding the method to other materials could benefit a host of applications in architectural and structural glazing and beyond.

■ ASSOCIATED CONTENT

Supporting Information

The Supporting Information is available free of charge at https://pubs.acs.org/doi/10.1021/acsapm.1c01854.

Additional experimental details, materials, methods, and figures including additional photographs, nitrogen adsorption isotherms, pore size distributions, optical measurements, SEM micrographs, and data interpretation (PDF)

■ AUTHOR INFORMATION

Corresponding Author

Mahati Chintapalli − *PARC, a Xerox Company, Palo Alto, California 94304, United States;* orcid.org/0000-0003-0270-0257; Email: mchintap@parc.com

Authors

Stephen M. Meckler − *PARC, a Xerox Company, Palo Alto, California 94304, United States;* orcid.org/0000-0002-2119-8867

Gabriel Iftime − *PARC, a Xerox Company, Palo Alto, California 94304, United States*

Asritha Nallapaneni − *Advanced Light Source, Lawrence Berkeley National Laboratory, Berkeley, California 94720, United States; The University of Akron, Akron, Ohio 44325, United States*

Quentin Van Overmeere − *PARC, a Xerox Company, Palo Alto, California 94304, United States*

Barkev Keoshkerian − *PARC, a Xerox Company, Palo Alto, California 94304, United States*

Eli Bulger − *PARC, a Xerox Company, Palo Alto, California 94304, United States*

Alec S. Ho − *PARC, a Xerox Company, Palo Alto, California 94304, United States;* orcid.org/0000-0003-1373-5332

Chenhui Zhu − *Advanced Light Source, Lawrence Berkeley National Laboratory, Berkeley, California 94720, United States*

Jessy B. Rivest − *PARC, a Xerox Company, Palo Alto, California 94304, United States*

Complete contact information is available at: https://pubs.acs.org/10.1021/acsapm.1c01854

Author Contributions

The manuscript was written through contributions of all authors. All authors have given approval to the final version of the manuscript.

Notes

The authors declare the following competing financial interest(s): PARC has filed a patent application based on the technology reported here.

■ ACKNOWLEDGMENTS

The information, data, or work presented herein was funded in part by the Advanced Research Projects Agency-Energy (ARPA-E), U.S. Department of Energy, under Award Number DE-AR0000734. The views and opinions of authors expressed herein do not necessarily state or reflect those of the United States Government or any agency thereof. Additional funding was provided by PARC, a Xerox Company. Beamline 7.3.3 is supported by the Director of the Office of Science, Office of Basic Energy Sciences, of the U.S. Department of Energy under Contract No. DE-AC02-05CH11231. Asritha Nallapaneni would like to thank the Advanced Light Source Doctoral Fellowship in Residence program for the financial support from the Lawrence Berkeley National Laboratory.

■ ABBREVIATIONS

SFRP, stable free radical polymerization; PDVB, polydivinylbenzene; RP, radical polymerization; DCP, dicumyl peroxide; AIBN, azobis(isobutyronitrile); NMP, *N*-methylpyrrolidinone; NLDFT, nonlocal density functional theory

■ REFERENCES

(1) Hunt, A. J. Light Scattering for Aerogel Characterization. *J. Non. Cryst. Solids* **1998**, *225*, 303−306.
(2) Zhao, L.; Strobach, E.; Bhatia, B.; Yang, S.; Leroy, A.; Zhang, L.; Wang, E. N. Theoretical and Experimental Investigation of Haze in Transparent Aerogels. *Opt. Express* **2019**, *27*, A39−A50.
(3) Jensen, K. I.; Schultz, J. M.; Kristiansen, F. H. Development of Windows Based on Highly Insulating Aerogel Glazings. *J. Non. Cryst. Solids* **2004**, *350*, 351−357.
(4) Emmerling, A.; Petricevic, R.; Beck, A.; Wang, P.; Scheller, H.; Fricke, J. Relationship between Optical Transparency and Nanostructural Features of Silica Aerogels. *J. Non. Cryst. Solids* **1995**, *185*, 240−248.
(5) Apte, J.; Arasteh, D. *Window-Related Energy Consumption in the US Residential and Commercial Building Stock*; Lawrence Berkeley National Laboratory: Berkeley, CA, 2006.
(6) Strobach, E.; Bhatia, B.; Yang, S.; Zhao, L.; Wang, E. N. High Temperature Stability of Transparent Silica Aerogels for Solar Thermal Applications. *APL Mater.* **2019**, *7*, 081104.
(7) Thapliyal, P. C.; Singh, K. Aerogels as Promising Thermal Insulating Materials: An Overview. *J. Mater.* **2014**, *2014*, 1.
(8) Strobach, E.; Bhatia, B.; Yang, S.; Zhao, L.; Wang, E. N. High Temperature Annealing for Structural Optimization of Silica Aerogels in Solar Thermal Applications. *J. Non-Cryst. Solids* **2017**, *462*, 72−77.
(9) Soleimani Dorcheh, A.; Abbasi, M.H. Silica Aerogel; Synthesis, Properties and Characterization. *J. Mater. Process. Technol.* **2008**, *199*, 10−26.
(10) Vivod, S. L.; Meador, M. A. B.; Pugh, C.; Wilkosz, M.; Calomino, K.; McCorkle, L. Toward Improved Optical Transparency of Polyimide Aerogels. *ACS Appl. Mater. Interfaces* **2020**, *12*, 8622−8633.
(11) Meador, M. A. B.; Malow, E. J.; Silva, R.; Wright, S.; Quade, D.; Vivod, S. L.; Guo, H.; Guo, J.; Cakmak, M. Mechanically Strong, Flexible Polyimide Aerogels Cross-Linked with Aromatic Triamine. *ACS Appl. Mater. Interfaces* **2012**, *4*, 536−544.
(12) Downey, J. S.; McIsaac, G.; Frank, R. S.; Stöver, H. D. H. Poly(Divinylbenzene) Microspheres as an Intermediate Morphology between Microgel, Macrogel, and Coagulum in Cross-Linking Precipitation Polymerization. *Macromolecules* **2001**, *34*, 4534−4541.
(13) Hawker, C. J.; Bosman, A. W.; Harth, E. New Polymer Synthesis by Nitroxide Mediated Living Radical Polymerizations. *Chem. Rev.* **2001**, *101*, 3661−3688.
(14) Ide, N.; Fukuda, T. Nitroxide-Controlled Free-Radical Copolymerization of Vinyl and Divinyl Monomers. 2. Gelation. *Macromolecules* **1999**, *32*, 95−99.
(15) Gao, H.; Matyjaszewski, K. Synthesis of Functional Polymers with Controlled Architecture by CRP of Monomers in the Presence of Cross-Linkers: From Stars to Gels. *Prog. Polym. Sci.* **2009**, *34*, 317−350.
(16) Keoshkerian, B.; Georges, M.; Quinlan, M.; Veregin, R.; Goodbrand, B. Polyacrylates and Polydienes to High Conversion by a Stable Free Radical Polymerization Process: Use of Reducing Agents. *Macromolecules* **1998**, *31*, 7559−7561.
(17) Debuigne, A.; Radhakrishnan, T.; Georges, M. K. Stable Free Radical Polymerization of Acrylates Promoted by α-Hydroxycarbonyl Compounds. *Macromolecules* **2006**, *39*, 5359−5363.
(18) Greszta, D.; Matyjaszewski, K. TEMPO-Mediated Polymerization of Styrene: Rate Enhancement with Dicumyl Peroxide. *J. Polym. Sci., Part A: Polym. Chem.* **1997**, *35*, 1857−1861.
(19) Odian, G. Living Radical Polymerization. In *Principles of Polymerization*, 4th ed.; John Wiley & Sons, Inc.: Hoboken, NJ, 2004; pp 325−328.
(20) Hexemer, A.; Bras, W.; Glossinger, J.; Schaible, E.; Gann, E.; Kirian, R.; MacDowell, A.; Church, M.; Rude, B.; Padmore, H. A SAXS/WAXS/GISAXS Beamline with Multilayer Monochromator. *J. Phys. Conf. Ser.* **2010**, *247*, 012007.
(21) Tamon, H.; Ishizaka, H. SAXS Study on Gelation Process in Preparation of Resorcinol-Formaldehyde Aerogel. *J. Colloid Interface Sci.* **1998**, *206*, 577−582.
(22) Yang, Y. Thermal Conductivity. In *Physical Properties of Polymers Handbook*; Mark, J. E., Ed.; Springer Science+Business Media, LLC: New York, 2007; pp 155−164.

https://doi.org/10.1021/acsapm.1c01854
ACS Appl. Polym. Mater. 2022, 4, 1565−1569